

Article

Preparation and Characterization of ZnS, CdS and HgS/Poly(methyl methacrylate) Nanocomposites

Johannes Z. Mbese and Peter A. Ajibade *

Department of Chemistry, University of Fort Hare, Private Bag X1314, Alice 5700, Eastern Cape, South Africa; E-Mail: jmbese@ufh.ac.za

* Author to whom correspondence should be addressed; E-Mail: pajibade@ufh.ac.za; Tel.: +27-406-022-055; Fax: +27-865-181-225.

Received: 26 May 2014; in revised form: 24 July 2014 / Accepted: 4 August 2014 /

Published: 5 September 2014

Abstract: The synthesis and characterization of ZnS/PMMA (poly(methyl methacrylate)), CdS/PMMA and HgS/PMMA nanocomposites are presented. Hexadecylamine (HDA)-capped ZnS, CdS and HgS nanoparticles were synthesized using dithiocarbamate single molecule precursors at 180 °C. FTIR (Fourier transform infrared spectroscopy) spectra measurement confirmed the dispersion of the metal sulfide nanoparticles in the PMMA matrices to form the metal sulfides/PMMA nanocomposites. Powder X-ray diffraction confirmed the presence of the amorphous PMMA in the nanocomposites. The ZnS and HgS particles were indexed to the cubic phase, while the CdS particles correspond to the hexagonal phase. Thermogravimetric analyses showed that the metal sulfide nanocomposites are thermally more stable than their corresponding precursor complexes. The TEM (Transmission electron microscope) analyses revealed that the ZnS nanoparticles have a particle size of 3–5 nm; the crystallite size of the CdS nanoparticles is 6–12 nm, and HgS nanoparticles are 6–12 nm.

Keywords: ZnS; CdS; HgS; poly(methyl methacrylate); nanocomposites; synthesis; characterization

1. Introduction

Nanocomposites derived from nano-scale inorganic/organic particles that are dispersed in a polymer matrix homogeneously have attracted considerable attention [1–5]. The diverse properties of numerous

polymers to choose from are well documented, including both plastics and elastomers, which are the main two types of polymers [6]. Organic/inorganic hybrid materials offer highly interesting and versatile applications when incorporated with a polymer [7]. Among the inorganic/polymer nanocomposites, metal sulfides/polymer nanocomposites have been researched extensively due to their interesting optical, electrical and mechanical properties [8]. Their excellent physical and chemical properties in various fields, such as catalysis, sensors, solar cells, photo detectors, light emitting diodes and laser communication, have made them very attractive and promising materials [9]. The defense applications of nanocomposites have also been reviewed [10]. Semiconductor particles immobilized in a polymer matrix with nano-scale grain size show different properties relative to the same material in bulk form because of quantum size effects [11–13]. Many different synthetic approaches, like thermal evaporation, chemical bath deposition, chemical vapor deposition (CVD), laser ablation, hydrothermal, homogeneous precipitation in an organic matrix, sonochemical and sol–gel methods, have been employed for the synthesis of metal sulfide nanoparticles [14–17]. The single-source precursor method has been demonstrated as a versatile method to synthesize several kinds of high-quality metal sulfide nanomaterials [18–20]. In this work, ZnS, CdS and HgS/poly(methyl methacrylate) (PMMA) nanocomposites were synthesized by embedding the metal sulfide nanoparticles into the PMMA matrix [21,22]. The optical and structural properties of nanocomposites were studied by FTIR (Fourier transform infrared spectroscopy), TGA (Thermogravimetric analyses), XRD (X-ray diffraction), SEM (scanning electron microscopy) and TEM (Transmission electron microscopy).

2. Experimental Section

2.1. Materials

All manipulations of air-sensitive compounds were carried under inert atmosphere using standard Schlenk techniques. All chemicals and reagents are analytical grade and were used as purchased from Sigma-Aldrich (St. Louis, MO, USA). ZnS, CdS and HgS were prepared from (*N*-phenyl-*N,N*-ethyl phenyl dithiocarbamate)M(II) complexes [23].

2.2. Synthesis of Metal Sulfides/PMMA Nanocomposites

The nanocomposites were prepared from their respective metal sulfide nanoparticles using a modified literature procedure [21,22]. In a typical experiment, 1.5 g of PMMA in 20 mL toluene were stirred for an hour. This was followed by the addition of a solution containing 0 and 3% (0.0 and 0.045 g) weight percent of ZnS nanoparticles in toluene. The mixture was heated and stirred vigorously. The resulting turbid solutions were poured onto Petri dishes and allowed to dry. White ZnS/PMMA nanocomposites were obtained. A similar procedure was used for the synthesis of CdS/PMMA and HgS/PMMA nanocomposites. The products were obtained in good yields of 85%–95%, with a thickness of 0.1–0.2 mm.

2.3. Characterization

Infrared spectra were recorded on a Perkin–Elmer (Waltham, MA, USA) 2000 FT-IR spectrometer. Powder X-ray diffraction patterns were recorded on a Bruker-D8 ADVANCE powder X-ray

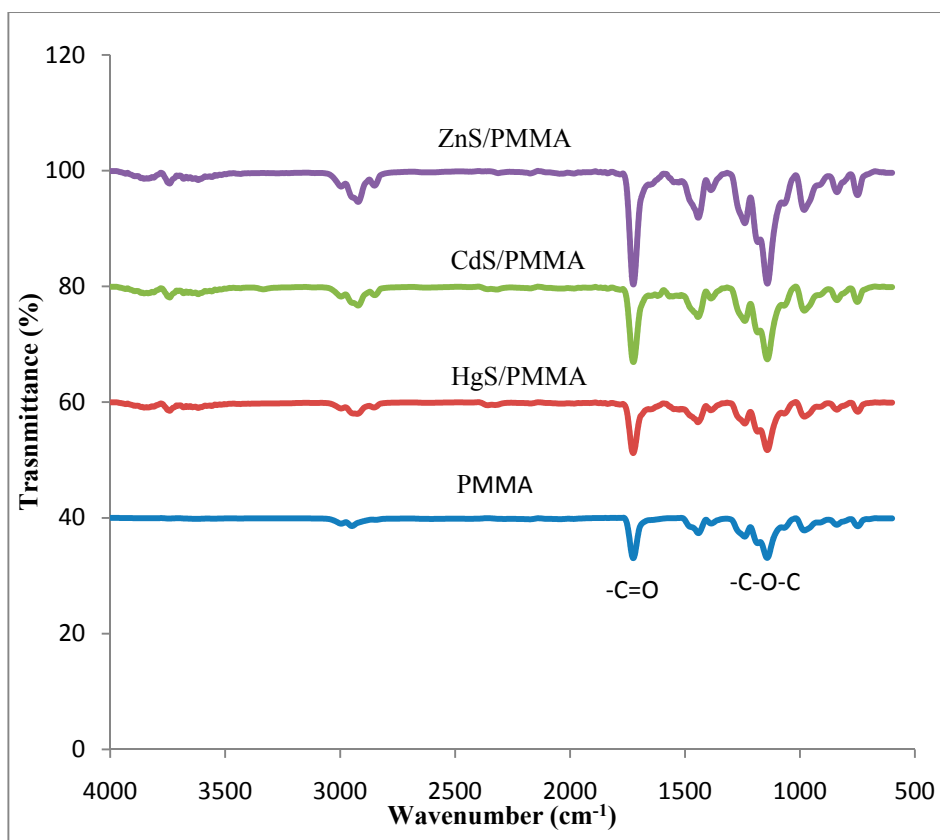
diffractometer (Bruker AXS GmbH, Karlsruhe, Germany) instrument operating at a voltage of 40 kV and a current of 30 mA with Cu $K\alpha$ radiation. TGA experiment was carried out on a Perkin Elmer thermogravimetric analyzer (TGA 7) fitted with a thermal analysis controller (TAC 7/DX). The SEM images were obtained in a Jeol (Tokyo, Japan), JSM-6390 LV apparatus, using an accelerating voltage between 15 and 20 kV. Energy dispersive spectra were processed using energy dispersive X-ray analysis (EDX) attached to the instrument with Noran System six software. The TEM images were obtained using a ZEISS (Oberkochen, Germany) Libra 120 electron microscope operated at 120 kV. The samples were prepared by placing a drop of a solution of the sample in toluene on a carbon-coated copper grid (300 mesh, agar). Images were recorded on a MegaView G2 camera using iTEM Olympus software (Olympus, Münster, Germany).

3. Results and Discussion

3.1. Infrared Spectra Studies

FTIR spectra of the PMMA (Figure 1) showed C–H stretching vibration at 2977 cm^{-1} , a strong C=O peak around 1730 cm^{-1} and C–O–C stretching and deformation vibration peaks at 1157, 1199 and 1265 cm^{-1} ; the peaks observed at 999 cm^{-1} and 858 cm^{-1} correspond to the bending vibrations of C–H, and the peak at 746 cm^{-1} is attributed to the vibrations of the polymer chains [4].

Figure 1. FTIR spectra of PMMA and the metal sulfide nanocomposites.



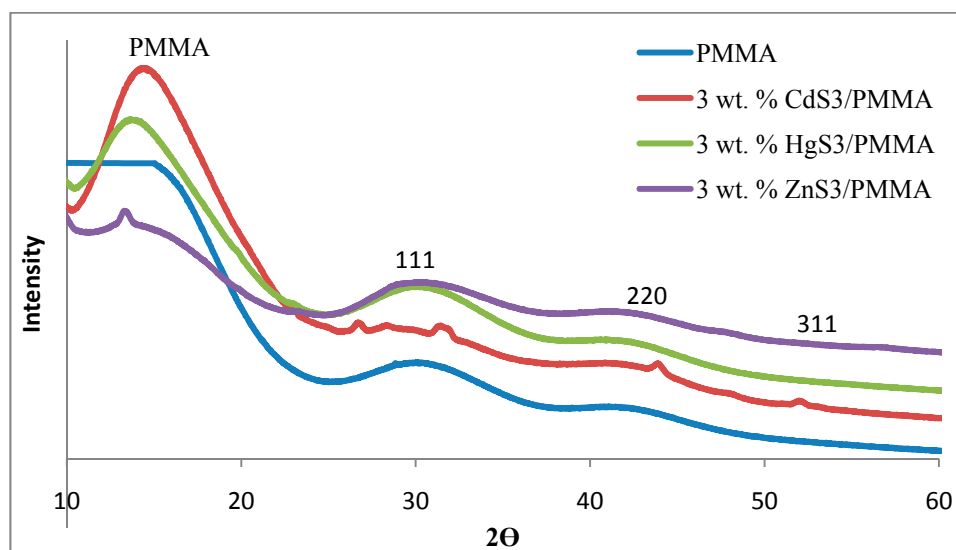
The spectra of pure PMMA and those of ZnS/PMMA, CdS/PMMA and HgS/PMMA nanocomposites are almost identical, which could be attributed to the metal sulfides crystallites being

in the pores of PMMA networks without disturbing the continuous three-dimensional network in the polymer matrices, and both are independent in their chemical behavior [24]. All of the stretching vibrations observed in the PPMA appeared in the nanocomposites with higher intensity. The van der Waals interactions between PMMA and the metal sulfide nanoparticles are very weak [25,26], and the amount of nanoparticles used does not affect the transparency of the nanocomposites [27]. The stretching vibrations around $405\text{--}265\text{ cm}^{-1}$ due to the M–S bond could not be observed, since it was beyond the extent of our measurement [28].

3.2. X-ray Diffraction Studies

Powder X-ray diffraction (XRD) patterns of free PMMA and the metal sulfides/PMMA nanocomposites are shown in Figure 2. The broad hump diffraction peak present in PMMA and the nanocomposites around $2\theta = 15^\circ$ is ascribed to amorphous PMMA [29]. In ZnS/PMMA nanocomposites' XRD patterns, the other peaks with 2θ values of 29.9° , 42.4° and 52.3° corresponded to the ZnS cubic phase assigned to the (111), (220) and (311) crystalline planes of ZnS, consistent with the literature data of JCPDS 5-0566 [30]. All of the XRD peaks of ZnS are relatively broad, which confirms the small size of ZnS nanoparticles in the composite.

Figure 2. XRD diffraction patterns PMMA, ZnS/PMMA, CdS/PMMA and HgS/PMMA nanocomposites.

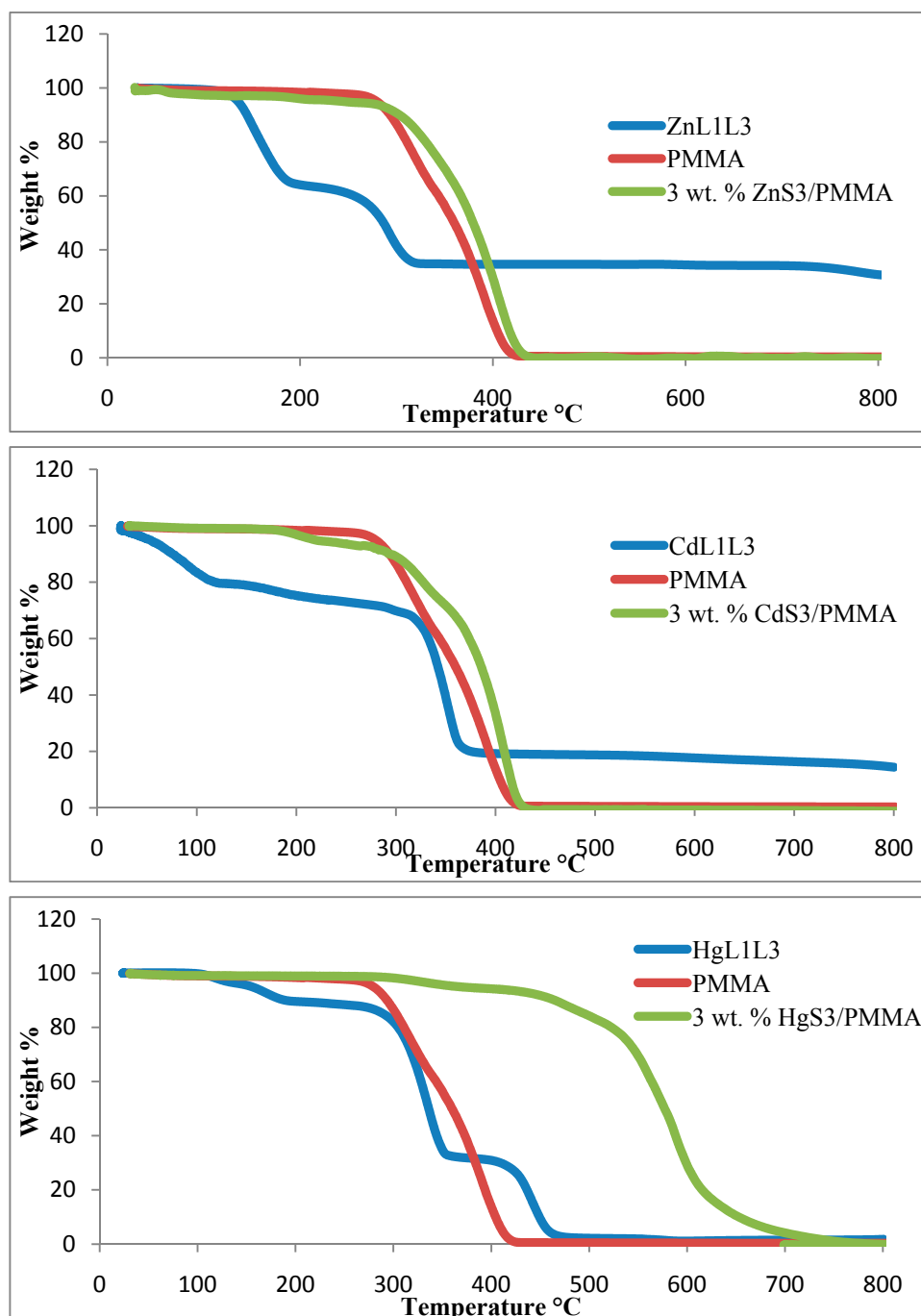


The average particle size calculated from the X-ray diffraction study using the Debye–Scherrer formula [31] was found to be 1.08 nm. The XRD pattern of as-prepared CdS/PMMA nanocomposites and PMMA also indicate the characteristic peaks of the cubic crystal structure corresponding to (111), (220) and (311) reflections. The broad XRD peaks indicate the small crystallite size of the CdS particles in the nanocomposites. A calculated average particle size of 2.3 nm was obtained from the X-ray diffraction study using Debye–Scherrer formula. The XRD patterns of HgS/PMMA nanocomposites shows three characteristic peaks at $2\theta = 29.5^\circ$, 42.5° and 52.5° , corresponding to Miller indices (111), (220) and (311) [32–34]. An average particle size of 1.8 nm has been calculated from X-ray diffraction for HgS.

3.3. Thermogravimetric Analysis of the Metal Sulfides/PMMA Nanocomposites

Figure 3 shows the TGA decomposition curves for the metal sulfides/PMMA nanocomposites, pure PMMA matrix and their respective precursor complexes. The major decomposition of CdS/PMMA nanocomposites occurs at about 272–435 °C, indicating that the thermal stability of CdS/PMMA nanocomposites, which could be ascribed to strong interactions between the CdS nanoparticles and the PMMA polymer matrices.

Figure 3. TGA curves for precursor complexes, pure PMMA and their corresponding metal sulfides/PMMA nanocomposites.



The residue observed could be ascribed to the presence of CdS nanoparticles in PMMA matrix. The thermal stability of CdS/PMMA nanocomposites in comparison to the precursor complex might be due to the combination of CdS nanoparticles in the polymer matrix, which yielded a stronger binding force due to the interactions between CdS nanoparticles and the polymer backbone [35,36]. The TGA curve for HgS/PMMA nanocomposites shows outstanding thermal stability compared to the PMMA matrix and precursor complex, confirming that the nanoparticle-polymer interaction is strong. The major decomposition occurs at about 300–750 °C, accompanied with about a 90% weight loss of the nanocomposites. This may be due to the volatilization of HgS at the high temperature, leaving a small amount of HgS/PMMA nanocomposite residue. Since only 3 wt% of metal sulfide nanoparticles is present in the nanocomposites, it could be expected that the interaction between the PMMA matrix and the metal sulfide nanoparticles increases with the increase in the amount of nanoparticles dispersed into the PMMA matrix [37]. The main degradation step of ZnS/PMMA nanocomposites is around 264–427 °C and has more thermal stability than pure PMMA, which can be due to the amount of ZnS nanoparticles embedded into the PMMA matrix. This clearly indicates that the thermal stability for the ZnS/PMMA nanocomposites has been improved significantly at a higher decomposition temperature compared to pure PMMA [38].

3.4. SEM and EDX Studies of the Nanocomposites

The SEM micrograph and EDX spectrum of the nanocomposites are presented in Figure 4. It shows spherical morphologies indicating that all ZnS nanoparticles are within PMMA matrices having spherical particles with a smooth surface and narrow, distributed particle sizes [39,40]. Energy-dispersive X-ray spectroscopy (EDX) showed improved Zn:S stoichiometry and reduced oxygen content in the spectra of ZnS/PMMA nanocomposites, confirming the presence of ZnS nanoparticles in PMMA matrix [41].

The CdS/PMMA composite confirms the existence of CdS nanoparticles, which are homogeneously dispersed in the PMMA matrix [42]. It shows that PMMA played an important role in controlling the size and mono-dispersion of CdS nanoparticles. The absence of agglomerates is ascribed to the role played by the PMMA matrix, because it is adsorbed onto the different planes of the incipient CdS nuclei, and it prevents the particles from agglomeration [43]. The EDX spectra of CdS/PMMA nanocomposites also reveal that the prepared nanocomposites are mainly composed of Cd and S, confirming the presence of CdS nanoparticles in the PMMA matrix [44].

The micrograph of HgS/PMMA nanocomposites shows evenly distributed spherical particles with agglomeration. The EDX spectrum reveals that the prepared nanocomposites are mainly composed of Hg and S, confirming the presence of HgS nanoparticles within the host PMMA matrix. The EDX of all nanocomposites reveals the presence of traces of elements, like C, O and Au. Carbon and oxygen are observed, possibly due to the use of carbon tape and retained solvent after the deposition step [45]. The intense Au peaks are due to the gold and palladium coating, which was used to overcome the charging of the samples.

Figure 4. SEM images and EDX for ZnS/PMMA (a,b,c); CdS/PMMA (d,e,f) and HgS/PMMA (g,h,i) nanocomposites.

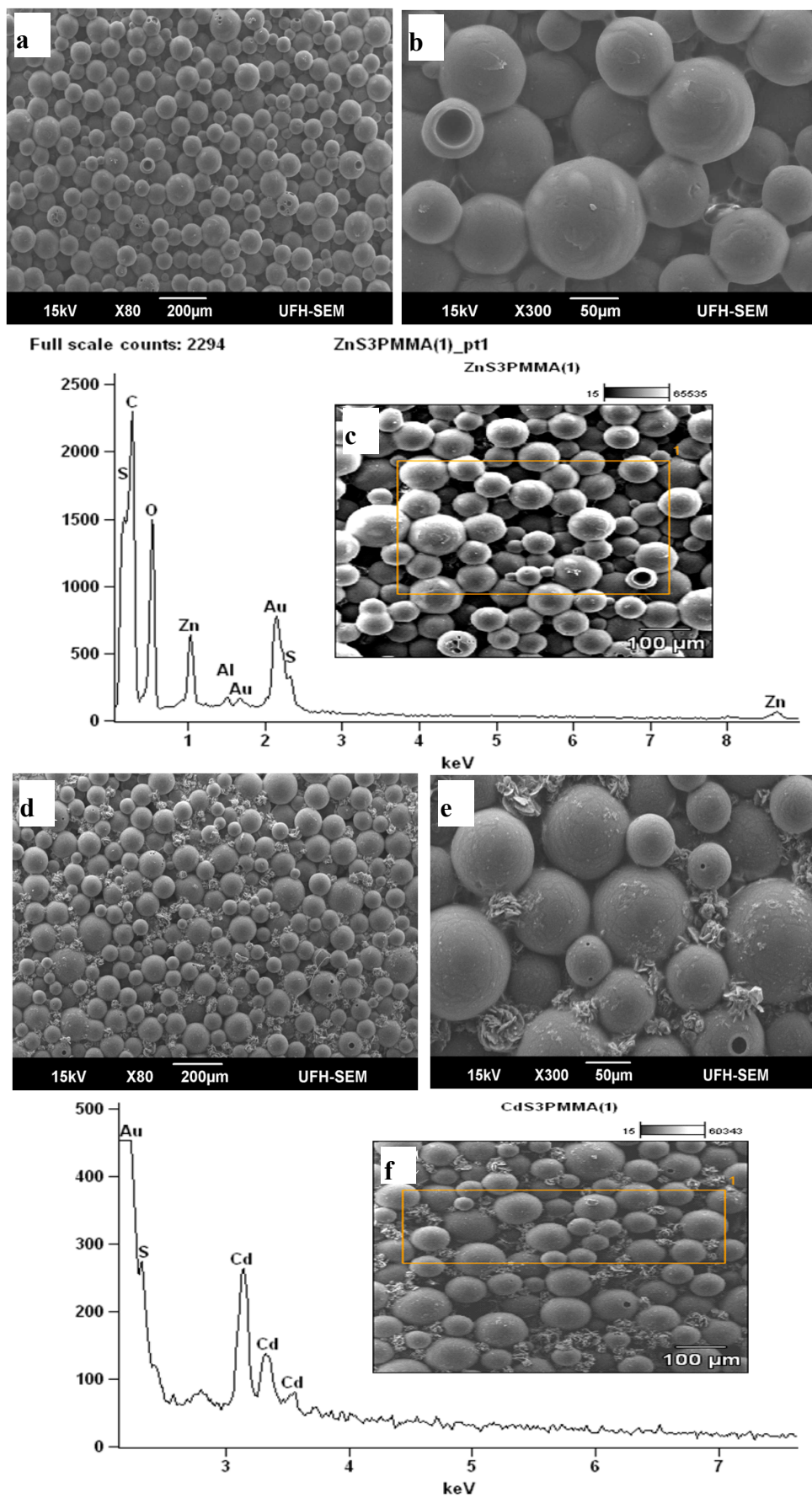
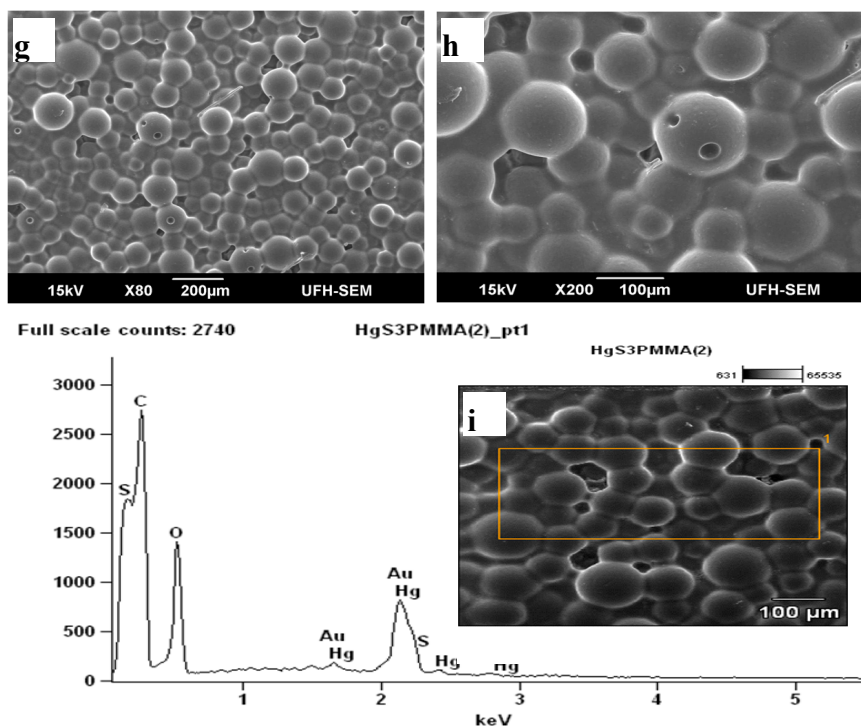


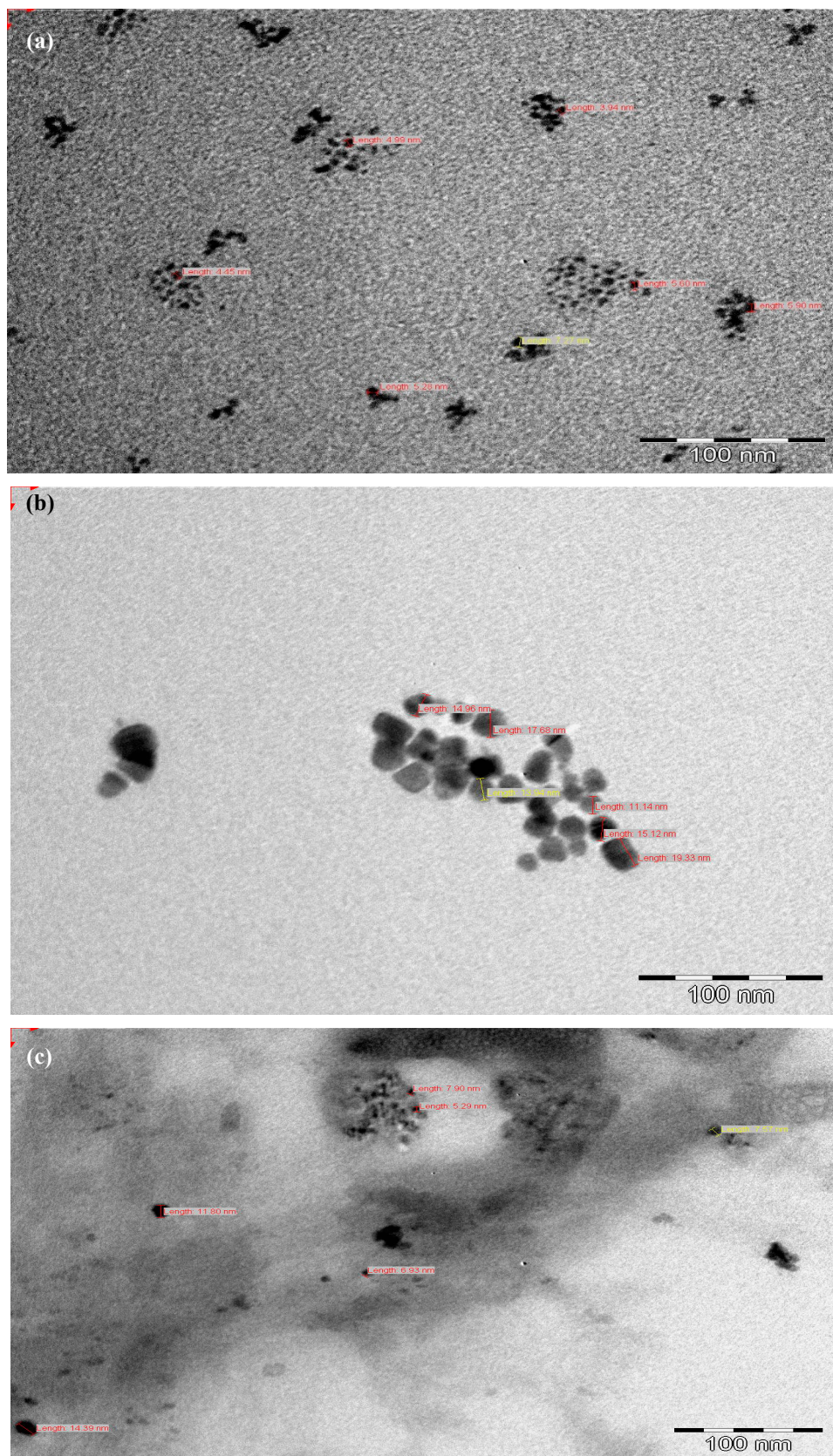
Figure 4. Cont.



3.5. TEM Studies of Nanocomposites

The TEM image of ZnS/PMMA nanocomposites (Figure 5) indicates that the particles are monodispersed in PMMA, although there is a small agglomeration. The TEM picture shows nanocomposites having a narrow size distribution of the particles ranging from 3 to 5 nm, which is in agreement with those estimated from XRD. The image also indicates that the ZnS nanoparticles have their size in the nano regime, even after being dispersed to the PMMA matrix [46–48]. The TEM image of CdS/PMMA nanocomposites shows that CdS particles were homogeneously dispersed in the PMMA polymer matrix with a standard deviation of about two. The particle sizes found in TEM are slightly different from those obtained from the XRD. This slight difference in particle size estimation through the XRD and TEM is due to the intrinsic twinning and dislocations present in the lattice of the sample. The CdS particles become agglomerated. A TEM image of HgS/PMMA nanocomposites prepared from HgS nanoparticles is shown in Figure 5. The TEM image shows nanoparticles in the 5–12 nm range. All of the transmission electron microscopy (TEM) images confirm the nanocrystalline nature of the ZnS, CdS and HgS nanocomposites studied.

Figure 5. TEM micrographs for ZnS/PMMA (a); CdS/PMMA (b) and HgS/PMMA (c).



4. Conclusions

Metal sulfide nanoparticles/poly(methyl methacrylate) nanocomposites formulated as ZnS/PMMA, CdS/PMMA, and HgS/PMMA were synthesized from their metal sulfide nanoparticles in the presence of the poly(methyl methacrylate) matrix. All of the prepared nanocomposites showed a reasonably good interaction between metal sulfide nanoparticles and the PMMA matrix. The PMMA acted as a good host matrix, since it did not affect the shape and properties of the metal sulfide nanoparticles dispersed to it, but provided combinations of functionalities. Metal sulfide nanoparticles in the PMMA matrix showed enhanced thermally stability as compared to pure PMMA, but less thermally stability compared to their respective metal dithiocarbamate complexes, which were used during metal sulfide nanoparticles syntheses. The CdS/PMMA revealed relatively broad XRD peaks, which indicate that CdS nanoparticles in the nanocomposites were small size. The average particle size of the metal sulfide nanoparticles in the PMMA ranges from 3 to 11 nm.

Acknowledgments

The authors gratefully acknowledge financial support from Govan Mbeki Research and Development Centre), University of Fort Hare, South Africa, and the Electricity Supply Commission, South Africa tertiary education support program.

Author Contributions

The authors contributed equally to this manuscript.

Conflicts of Interest

The authors declare no conflict of interest.

References

1. Carotenuto, G.; Nicolais, L.; Perlo, P.; Martorana, B. Method of production of polymer/metal or metal sulphide composites which uses metal mercaptides. U.S. Patent 7329700, 20 December 2014.
2. Capezzuto, F.; Carotenuto, G.; Antolini, F.; Burrelli, E.; Palomba, M.; Perlo, P. New fluorescent polymeric nanocomposites synthesized by antimony dodecyl-mercaptide thermolysis in polymer. *Express Poly. Lett.* **2009**, *3*, 219–225.
3. Caseri, W. Nanocomposites of polymers and metals or semiconductors: Historical background and optical properties. *Macromol. Rap. Commun.* **2000**, *21*, 705–722.
4. Mthethwa, T.P.; Moloto, M.J.; de Vries, A.; Matabola, K.P. Properties of electrospun CdS and CdSe filled poly(methyl methacrylate) (PMMA) nanofibres. *Mater. Res. Bull.* **2011**, *46*, 569–575.
5. Dixit, M.; Gupta, S.; Mathur, V.; Rathore, K.S.; Sharma, K.; Saxena, N.S. Study of glass transition temperature of PMMA and CdS-PMMA composite. *Chalco. Lett.* **2009**, *6*, 131–136.
6. Jeon, I.Y.; Baek, J.B. Nanocomposites derived from polymers and inorganic nanoparticles. *Materials* **2010**, *3*, 3654–3674.

7. Kaltenhauser, V.; Rath, T.; Haas, W.; Torvisco, A.; Muller, S.K.; Friedel, B.; Kunert, B.; Saf, R.; Hofer, F.; Trimmel, G. Bismuth sulphide-polymer nanocomposites from a highly soluble bismuth xanthate precursor. *J. Mater. Chem. C* **2013**, *1*, 7825–7832.
8. Zhang, C.Q.; Sun, J.; Wang, W.; Yang, Q.B.; Li, Y.X.; Du, J.S. Facile method to prepare metal sulfide (Ag₂S, CuS, PbS) nanoparticles grown on surface of polyacrylonitrile nanofibre and their optical properties. *Chem. Res. Chin. Univ.* **2012**, *28*, 534–538.
9. Ranjbar, M.; Yousefi, M.; Nozari, R.; Sheshmani, S. Synthesis and characterization of cadmium-thioacetamide nanocomposites using a facile sonochemical approach: A precursor for producing Cds nanoparticles via thermal decomposition. *Int. J. Nanosci. Nanotechnol.* **2013**, *9*, 203–212.
10. Kurahatti, R.V.; Surendranathan, A.O.; Kori, S.A.; Singh, N.; Kumar, A.V.R.; Srivastava, S. Defence applications of polymer nanocomposites. *Def. Sci. J.* **2010**, *60*, 551–563.
11. Jayanthi, K.; Chawla, S.; Chander, H.; Haranath, D. Structural, optical and photoluminescence properties of ZnS: Cu nanoparticle thin films as a function of dopant concentration and quantum confinement effect. *Cryst. Res. Technol.* **2007**, *42*, 976–982.
12. O'Brien, P.; Peakett, N.L. Nanocrystalline semiconductors: Synthesis, properties, and perspectives. *Chem. Mater.* **2001**, *13*, 3843–3858.
13. Singh, C.P.; Bindra, K.S.; Oak, S.M. Nonlinear optical studies in semiconductor-doped glasses under femtosecond pulse excitation. *Pramana J. Phys.* **2010**, *75*, 1169–1173.
14. Khaorapong, N.; Ontam, A.; Ogawa, M. Very slow formation of copper sulfide and cobalt sulfide nanoparticles in montmorillonite. *Appl. Clay Sci.* **2011**, *51*, 82–186.
15. Indulal, C.R.; Kumar, G.S.; Vaidyan, A.V.; Raveendran, R. Oxide nanostructures: Characterisations and optical bandgap evaluations of cobalt manganese and nickel at different temperatures. *J. Nano Electron. Phys.* **2011**, *3*, 170–178.
16. Sinkó, K.; Szabó, G.; Zrínyi, M. Liquid-phase synthesis of cobalt oxide nanoparticles. *J. Nanosci. Nanotechnol.* **2011**, *11*, 1–9.
17. Ezema, F.I. Preparation and optical characterization of chemical bath deposited CdCoS₂ Thin Films. *J. Appl. Sci.* **2006**, *6*, 1827–1832.
18. Onwudiwe, D.C.; Ajibade, P.A. ZnS, CdS and HgS nanoparticles via alkyl-phenyl dithiocarbamate complexes as single source precursors. *Int. J. Mol. Sci.* **2011**, *12*, 5538–5551.
19. Zhang, Y.C.; Chen, W.W.; Hu, X.Y. Controllable synthesis and optical properties of Zn-doped CdS nanorods from single-source molecular precursors. *Cryst. Growth Des.* **2007**, *7*, 580–586.
20. Plante, I.J.L.; Zeid, T.W.; Yang, P.; Mokari, T. Synthesis of metal sulfide nanomaterials via thermal decomposition of single-source precursors. *J. Mater. Chem.* **2010**, *20*, 6612–6617.
21. Prabhu, S.G.; Pattabi, B.M. Incorporation of acetoacetanilide crystals in host PMMA polymer matrix and characterizations of the hybrid composite. *J. Mine. Mater. Charact. Eng.* **2012**, *11*, 519–527.
22. Agrawal, S.; Patidar, D.; Saxena, N.S. Glass transition temperature and thermal stability of ZnS/PMMA nanocomposites. *Phase Trans.* **2011**, *84*, 888–900.
23. Nicolais, L.F.; Carotenuto, G. Synthesis of polymer-embedded metal, semimetal, or sulfide clusters by thermolysis of mercaptide molecules dissolved in polymers. *Recent Pat. Mater. Sci.* **2008**, *1*, 1–11.

24. Agarwal, S.; Patidar, D.; Saxena, N.S. Effect of ZnS nanofiller and temperature on mechanical properties of poly (methyl methacrylate). *J. Appl. Polym. Sci.* **2012**, *123*, 2431–2438.
25. Li, Z.; Zhang, J.; Du, J.; Mu, T.; Liu, Z.; Chen, J.; Han, B. Preparation of cadmium sulfide/poly(methyl methacrylate) composites by precipitation with compressed CO₂. *J. Appl. Polym. Sci.* **2004**, *94*, 1643–1648.
26. Guan, C.; Lu, C.; Cheng, Y.; Song, S.; Yang, B. A facile one-pot route to transparent polymer nanocomposites with high ZnS nanophase contents via *in situ* bulk polymerization. *J. Mater. Chem.* **2009**, *19*, 617–621.
27. He, R.; Qian, X.F.; Yin, J.; Bian, L.J.; Xi, H.A.; Zhu, Z.K. *In situ* synthesis of CdS/PVK nanocomposites and their optical properties. *Mater. Lett.* **2003**, *57*, 1351–1354.
28. Yao, J.; Zhao, G.; Wang, D.; Han, G. Solvothermal synthesis and characterization of CdS nanowires/PVA composite films. *Mater. Lett.* **2005**, *59*, 3652–3655.
29. Borah, J.P.; Sarma, K.C. Photo-physical properties of ZnS/PVA nanocrystals. *Optoelectron. Adv. Mater. Rapid Commun.* **2009**, *3*, 891–898.
30. Bhaiswar, J.B.; Salunkhe, M.Y.; Dongre, S.P. Synthesis, characterization and thermal, electrical study of CdS-polyaniline nanocomposite via oxidation polymerization. *Int. J. Sci. Res. Public.* **2013**, *3*, 1–4.
31. Lee, H.L.; Mohammed, I.A.; Belmahi, M.; Assouar, M.B.; Rinnert, H.; Alnot, M. Thermal and optical properties of CdS nanoparticles in thermotropic liquid crystal monomers. *Materials* **2010**, *3*, 2069–2086.
32. Mehta, S.K.; Kumar, S.; Chaudhary, S.; Bhasin, K.K. Nucleation and growth of surfactant-passivated CdS and HgS nanoparticles: Time-dependent absorption and luminescence profiles. *Nanoscale* **2010**, *2*, 145–152.
33. Oshal, F.; Mossalayi, H. Effect of matrices on size and morphology of HgS nanoparticles. *Der Pharma Chemica* **2010**, *2*, 33–37.
34. Jang, J.; Kim, S.; Lee, K.J. Fabrication of CdS/PMMA core/shell nanoparticles by dispersion mediated interfacial polymerization. *Chem. Commun.* **2007**, 2689–2691.
35. Kuljanin, J.; Marinović-Cincović, M.; Stojanović, Z.; Krklješ, A.; Abazović, N.D.; Comor, M.I. Thermal degradation kinetics of polystyrene/cadmium sulfide composites. *Polym. Degrad. Stab.* **2009**, *94*, 891–897.
36. Marimuthu, G.; Ramalingam, K.; Rizzoli, C.; Arivanandhan, M. Solvothermal preparation of nano-*b*-HgS from a precursor, bis(dibenzylthiocarbamate)mercury(II). *J. Nanopart. Res.* **2012**, *14*, 1–11.
37. Tamrakar, R.; Ramrakhiani, M.; Chandra, B.P. Effect of capping agent concentration on photophysical properties of zinc sulfide nanocrystals. *Open Nanosc. J.* **2008**, *2*, 12–16.
38. Lee, S.J.; Kim, K.N.; Bae, P.K.; Chang, J.H.; Kim, Y.R.; Park, J.K. Sonication treatment of CdTe/CdS semiconductor nanocrystals and their bio-application. *Chem. Commun.* **2008**, *43*, 5574–5576.
39. Wei, S.; Sampathi, J.; Guo, Z.; Anumandla, N.; Rutman, D.; Kucknoor, A.; James, L.; Wang, A. Nanoporous poly(methyl methacrylate)-quantum dots nanocomposite fibers toward biomedical applications. *Polymer* **2011**, *52*, 5817–5829.

40. Liu, S.; Zhang, H.; Swihart, M.T. Spray pyrolysis synthesis of ZnS nanoparticles from a single-source precursor. *Nanotech.* **2009**, *20*, 1–8.
41. Jothi, N.S.N.; Gunaseelan, R.; Raj, T.M.; Sagayaraj, P. Investigation on mild condition preparation and structural, optical and thermal properties of PVP capped CdS nanoparticles. *Arch. Appl. Sci. Res.* **2012**, *4*, 1723–1730.
42. Barman, B.; Sarma, K.C. Luminescence properties of ZnS quantum dots embedded in polymer matrix. *Chalc. Lett.* **2011**, *8*, 171–176.
43. Sharma, R. Optical studies of CdS:Mn nanoparticles. *Luminescence* **2012**, *27*, 501–504.
44. Sharma, M.; Kumara, S.; Pandey, O.P. Photo-physical and morphological studies of organically passivated core-shell ZnS nanoparticles. *Dig. J. Nanomater. Biostruct.* **2008**, *3*, 189–197.
45. Tomar, A.K.; Mahendia, S.; Kumar, S. Structural characterization of PMMA blended with chemically synthesized PANi. *Adv. Appl. Sci. Res.* **2011**, *2*, 65–71.
46. Hashmi, L.; Sana, P.; Malik, M.M.; Siddiqui, A.H.; Qureshi, M.S. Novel fork architectures of Ag₂S nanoparticles synthesized through in-situ self-assembly inside chitosan matrix. *Nano Hybrids* **2012**, *1*, 23–43.
47. Amah, A.N.; Echi, I.M.; Kalu, O. Influence of polyvinyl alcohol and alpha-methacrylic acid as capping agents on particle size of ZnS nanoparticles. *Appl. Phys. Res.* **2012**, *4*, 26–34.
48. Liu, L.; Zheng, Z.; Wang, X. Preparation and properties of polythiourethane/ZnS nanocomposites with high refractive index. *J. Appl. Polym. Sci.* **2010**, *117*, 1978–1983.

© 2014 by the authors; licensee MDPI, Basel, Switzerland. This article is an open access article distributed under the terms and conditions of the Creative Commons Attribution license (<http://creativecommons.org/licenses/by/3.0/>).